Applied Radiation and Isotopes 190 (2022) 110507

Contents lists available at ScienceDirect

Applied Radiation and Isotopes

journal homepage: www.elsevier.com/locate/apradiso

Half-life measurement of ^{44}Sc and ^{44m}Sc

M. Teresa Durán [a,*], Frédéric Juget [a], Youcef Nedjadi [a], Claude Bailat [a], Pascal V. Grundler [b], Zeynep Talip [b], Nicholas P. van der Meulen [b,c], Pierluigi Casolaro [d], Gaia Dellepiane [d], Saverio Braccini [d]

[a] Institut de Radiophysique, Lausanne, Switzerland
[b] Center for Radiopharmaceutical Sciences ETH-PSI-USZ, Paul Scherrer Institute, Villigen-PSI, Switzerland
[c] Laboratory of Radiochemistry, Paul Scherrer Institute (PSI), Villigen-PSI, Switzerland
[d] Albert Einstein Center for Fundamental Physics (AEC), Laboratory for High Energy Physics (LHEP), University of Bern, Switzerland

ARTICLE INFO

Keywords:
^{44}Sc
^{44m}Sc
Half-life
Ionization chamber
Gamma-spectrometry
Nuclear data

ABSTRACT

The half-lives of ^{44}Sc and ^{44m}Sc were measured by following their decay rate using several measurement systems: two ionization chambers and three γ-spectrometry detectors with digital and/or analogue electronics. For ^{44}Sc, the result was the combination of seven half-life values giving a result of 4.042(7) h, which agrees with the last reported value of 4.042(3) h and confirms the near to 2% deviation from the recommended half-life of 3.97(4) h. Scandium-44 is present as an impurity in the production of ^{44}Sc by cyclotron proton irradiation. Its half-life was determined by measurements performed a few days after End of Bomardment (EoB), so that the ^{44}Sc decayed down to a negligible level. Seven measurements were combined to obtain an average of 58.7(3) h, which is in agreement with the recommended value of 58.6(1) h.

1. Introduction

^{44}Sc decays by β^+ emission (94.27(5) %) and electron capture (5.73 (5) %) to excited states of ^{44}Ca (Browne, 2004). It is a promising radionuclide to be used for high-resolution positron emission tomography (PET). Its ability to be combined with DOTA-derivative biomolecules and a longer half-life than most commonly-used radionuclides for PET imaging, such as ^{68}Ga ($T_{1/2}$ = 68 min) and ^{18}F ($T_{1/2}$ = 1.83 h), make it an interesting candidate to be used for nuclear medicine diagnostics. ^{44}Sc potential applications cover pre-therapeutic imaging, radionuclide therapy response monitoring and dosimetry (Müller et al., 2013; van der Meulen, 2015; Singh et al., 2017 and Lima et al., 2021).

The production of ^{44}Sc can be carried out in a cyclotron via the ^{44}Ca (p,n)^{44}Sc nuclear reaction (Van der Meulen, 2020) or by using a ^{44}Ti/^{44}Sc generator. When produced in a cyclotron, a separation of ^{44}Sc from ^{44}Ca is performed (van der Meulen, 2015), yielding high radionuclidic and chemical purity. Only small amounts (<1%) of other Sc isotopes can be detected, such as ^{47}Sc and ^{48}Sc (due to the target isotopic composition) and the excited state ^{44m}Sc (due to the energy spectrum of the incident protons), as will be shown in this work.

A collaboration between the Paul Scherrer Institut (PSI), the Laboratory for High Energy Physics (LHEP) of the University of Bern (UniBern) and the Institut de Radiophysique (IRA) provided the framework for a precise activity measurement of cyclotron-produced ^{44}Sc sources as well as the determination of its half-life. This work was later used to perform the calibration of dose calibrators at UniBern and PSI (paper in preparation). Additionally, the determination of the ^{44m}Sc half-life was also performed due to its presence in the irradiated sample used as a source. Previous half-life measurements (Fig. 1) showed incompatible results for ^{44}Sc, such as 4.042(3) h (García-Toraño et al., 2016) and 3.97(4) h (Browne, 2004 and Chen et al., 2011), the latter being the DDEP (Decay Data Evaluation Projet) recommended value.

The measurements presented in this work resulted in 4.042(7) h for ^{44}Sc, which is in better agreement with the last published value by García-Toraño et al. (2016), and 58.7(3) h for ^{44m}Sc, which is in agreement within uncertainties with the recommended value by Chen et al. (2011) coming from Ravn (1969).

2. Source preparation

A^{44}CaO enriched target (97%, Trace Sciences International, USA) was irradiated with ~11 MeV protons to undergo the ^{44}Ca(p,n)^{44}Sc reaction. Scandium-44 was separated and concentrated using extraction and exchange resins (van der Meulen, 2015). All these procedures were

* Corresponding author.
E-mail address: teresa.duran@chuv.ch (M.T. Durán).

https://doi.org/10.1016/j.apradiso.2022.110507
Received 8 July 2022; Received in revised form 30 August 2022; Accepted 1 October 2022
Available online 6 October 2022

performed at PSI and two solutions with different activity concentrations were sent to IRA. An aliquot of the less concentrated solution, 17.8 (1) mg, was sent in an Eppendorf vial to UniBern for an additional half-life measurement, while another was kept at PSI for calibration of their γ-spectrometry detector.

Solutions M44Sc_PSI1 and M44Sc_PSI2, in the form of 25 μg g^{-1} $ScCl_3$ in 0.1M HCl, consisted of 70 MBq ^{44}Sc in 2 g and 2 GBq in 0.5 g respectively. The first solution was diluted by a factor $F_{dil} = 11$ and used to prepare two sources for half-life determination: a solid one, by deposition of a droplet into a plastic container that was left to dry, and an ampoule containing 3 g of solution. Two additional vials were prepared from a further dilution ($F_{dil} = 3.9$) to be measured on a high-resolution HPGe detector to determine the presence of impurities and to quantify them. The second solution, M44Sc_PSI2, was stored until the initial ^{44}Sc had decayed and the activity of the remaining ^{44m}Sc, at this point in equilibrium with its daughter ^{44}Sc, was low enough to allow its detection by the γ spectrometer without saturation issues. After a period of four days, two solid sources and an ampoule were prepared for ^{44m}Sc half-life measurement. Fig. 2 shows a scheme of source preparation and their use.

2.1. Impurity check

The impurity check was performed by γ-spectrometry. The two polyethylene vials containing the ^{44}Sc solution were measured with a high resolution HPGe detector over a period of 10 h, in order to assess the activity of ^{44m}Sc. Additionally, the ampoule from the solution M44Sc_PSI2 was measured several days after, on 30 November 2021 and 6 December 2021, in order to search for long half-life radionuclides that might be present in the solution.

The spectra revealed the ^{44m}Sc emissions signature, and its activity was calculated using the 271 keV line. For ^{44}Sc, the 1499 keV line was used to calculate its activity, taking into account the fact that part of the ^{44}Sc comes from the decay of ^{44m}Sc. The activity ratio ^{44m}Sc/^{44}Sc at the reference time is 0.00756(14).

Several additional impurities were found in the M44Sc_PSI2 spectrum (Fig. 3): ^{46}Sc, ^{47}Sc, ^{48}Sc and ^{88}Y. As the ^{44}Sc and ^{44m}Sc are in equilibrium at the beginning of the measurement (around 100 h to reach the equilibrium), the activity ratio of the impurities is given with respect to the ^{44m}Sc activity at the reference date, 23.86(55) kBq·g^{-1}, in Table 1.

The evolution of the impurity ratios is shown in Fig. 4 together with the timing of the half-life measurements and, in more detail, those of ^{44m}Sc. This plot helped evaluate the contribution of the impurities for each measurement and decide how these radionuclides should be taken into account on the fit functions, as will be shown later.

3. ^{44}Sc and ^{44m}Sc half-life measurements

The half-life of ^{44}Sc was determined by recording the decay with five different systems. Two ionization chambers were used, namely TCIR (transportable reference ionization chamber) and CIR (reference ionization chamber), as in Juget et al. (2016) and Durán et al. (2020, 2021). The first measured the sources at the site of production and the second one was used at IRA's laboratory. A $CeBr_3$ γ detector was also used to measure counting rates with two separate electronic chains: analogue and digital as in Durán et al. (2021). The source sent to UniBern was measured by HPGe γ-spectrometry.

^{44m}Sc was measured with the same systems except for the $CeBr_3$ with digital electronics that was substituted by a NaI well-type detector using the same digital electronic chain.

3.1. Measurements with the TCIR

At the beginning of this project, the first preliminary measurements of ^{44}Sc were carried out at the site of production (PSI) using the TCIR. TCIR is the transportable reference ionization chamber that IRA uses to perform quick and reliable activity measurements of many radioisotopes at the production sites: hospitals, clinics, accelerators, etc (Juget et al., 2018). A first measurement was carried out four months earlier, where 2055 points were recorded during 19 h on a first measurement and 9731 points during 92 h on a second one.

The current was recorded by the system's electrometer and a double exponential fit following equation (*1*) was performed to take into account the ^{44m}Sc induced current; its activity ratio over ^{44}Sc was estimated as 0.2% at the production time.

$$I(t) = I_{44}(0) \bullet e^{-\lambda_{44}\bullet t} \bullet F_{dec} + I_{44m}(0) \bullet \left[e^{-\lambda_{44m}\bullet t} + \frac{\lambda_{44}}{\lambda_{44} - \lambda_{44m}} \bullet \left(e^{-\lambda_{44m}\bullet t} - e^{-\lambda_{44}\bullet t} \right) \right] \quad (1)$$

The term for the decay of ^{44}Sc is corrected by the decay during the measurements using this factor, $F_{dec} = \frac{1-e^{-\lambda_{44}\bullet\Delta t}}{\lambda_{44}\bullet\Delta t}$, where Δt is the duration of the individual measurements. The term for the decay of ^{44m}Sc accounts for the fact that ^{44m}Sc itself decays to ^{44}Sc and at the time of the measurement the equilibrium was still not reached.

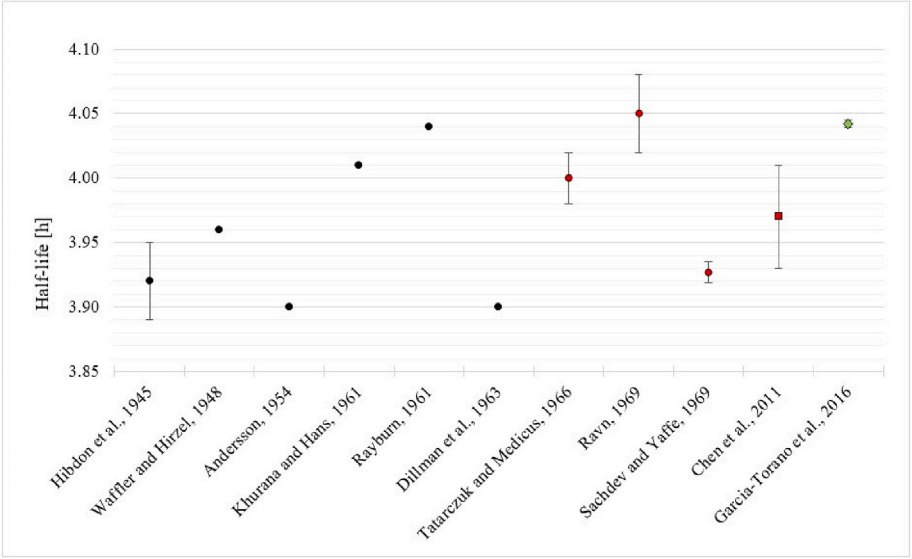

Fig. 1. Half-life values for ^{44}Sc. Red spots represent the three values (Tatarczuk and Medicus, 1966; Ravn, 1969 and Sachdev and Yaffe, 1969) used to obtain the recommended one (red square) (Browne, 2004 and Chen et al., 2011). The green diamond is the latest recorded value (García-Toraño et al., 2016) before publication of this article. The black spots refer to previous measurements (Hibdon et al., 1945; Waffler and Hirzel, 1948; Andersson, 1954; Khurana and Hans, 1961; Rayburn, 1961 and Dillman et al., 1963). (For interpretation of the references to colour in this figure legend, the reader is referred to the Web version of this article.)

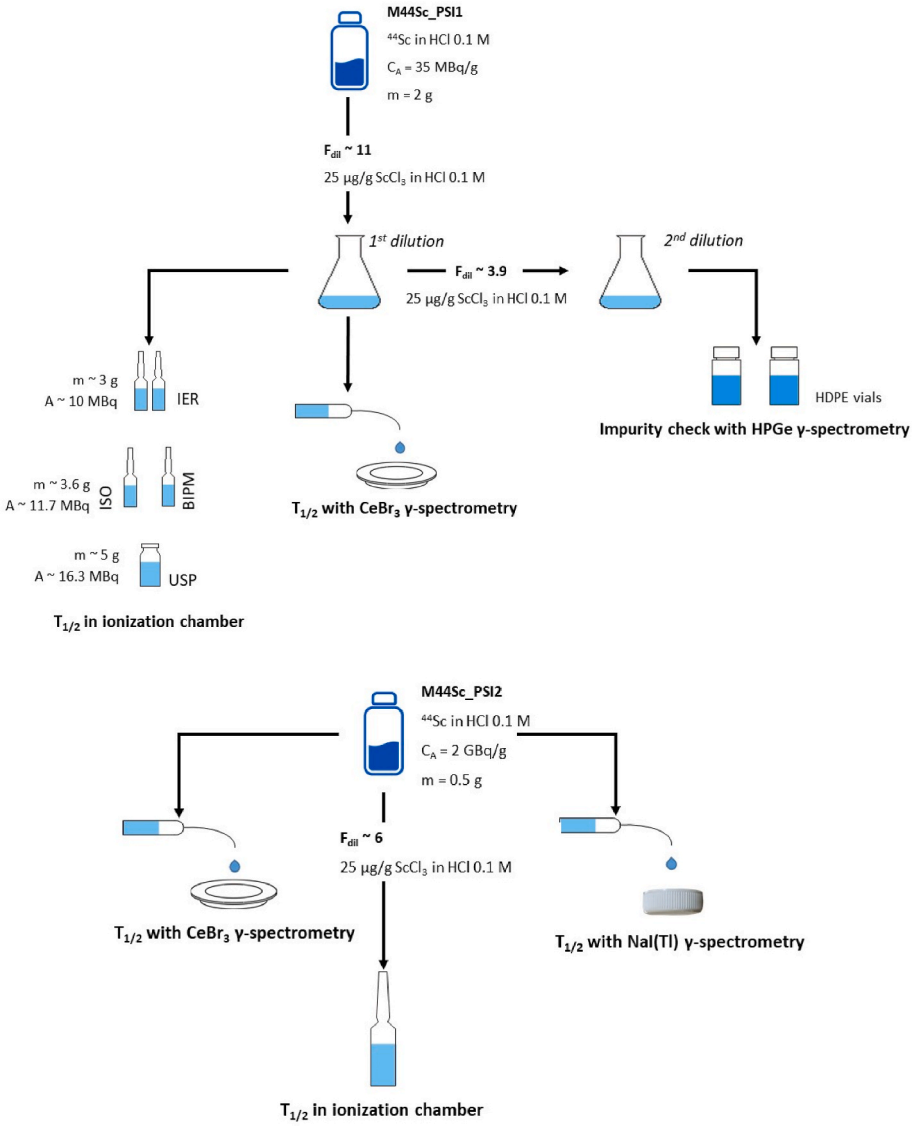

Fig. 2. Source preparation scheme from both solutions received from PSI.

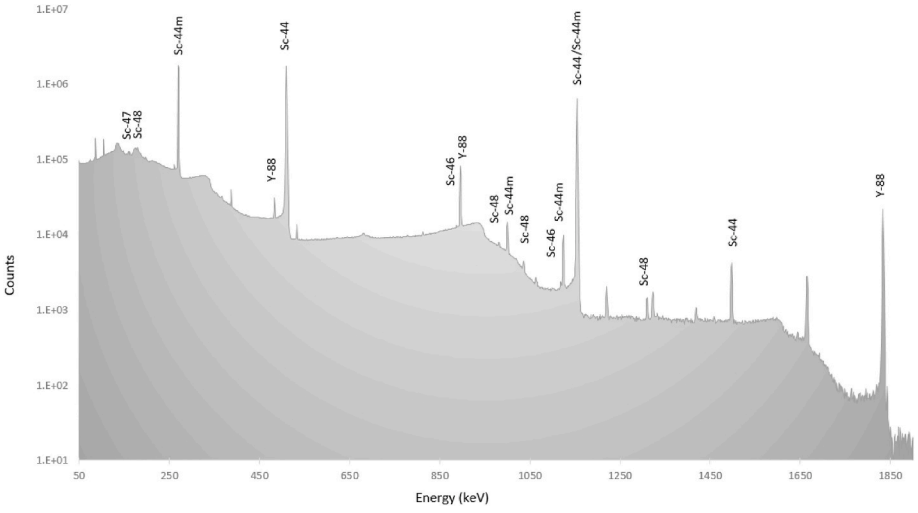

Fig. 3. γ spectrum measured on 6 December 2021 with the HPGe to search for long half-life impurities.

Table 1
Impurity ratio with respect to ^{44m}Sc for long half-life impurities.

Ratio	Value	Relative uncertainty on the ratio (%)
^{48}Sc/^{44m}Sc	0.00756	2.5
^{47}Sc/^{44m}Sc	0.00139	1.7
^{46}Sc/^{44m}Sc	0.0000056	4.4
^{88}Y/^{44m}Sc	0.000465	0.7

For the shorter first measurement (Fig. 5a), the ^{44m}Sc decay constant was kept fixed using the reference value of 58.6 days (Nucleide –LARA database), as we only intended to obtain the ^{44}Sc half-life due to the duration of the measurement (five times the expected ^{44}Sc half-life). Initial $I_{44}(0)$ and $I_{44m}(0)$ currents were kept as free parameters and the results were compatible with the estimated ratio of 0.2% from the initial measured current (at $t=0$). The result for ^{44}Sc half-life in this case is 4.038(3) h.

For the second and longer measurement (Fig. 5b), the value for the ^{44m}Sc half-life was also sought, as the duration of the measurement was long enough to allow its proper calculation (≈1.5 times the expected ^{44m}Sc half-life). Equation (*1*) was, again, used to perform the fit but, instead, keeping both decay constants as fit parameters. The values obtained for ^{44}Sc and ^{44m}Sc are 4.0391(8) h and 58.6(2) h, respectively.

To check the consistency of both fits, the first dataset was fitted again using the ^{44m}Sc decay constant obtained on the second fit instead of the reference value. The resultant value for ^{44}Sc half-life remained unchanged: 4.04 h.

At the time of the latter ^{44}Sc production (in November 2021), another source was measured on-site for a period of 73 h, providing 7843 points. Due to the presence of more impurities, the fit was performed with a four-exponential decay equation (2), also taking the decay during measurement as well as the impurity ratios found for ^{47}Sc and ^{48}Sc into account. These two radioisotopes were the most abundant impurities at the time of measurement, along with ^{44m}Sc, not yet in equilibrium with its ^{44}Sc daughter.

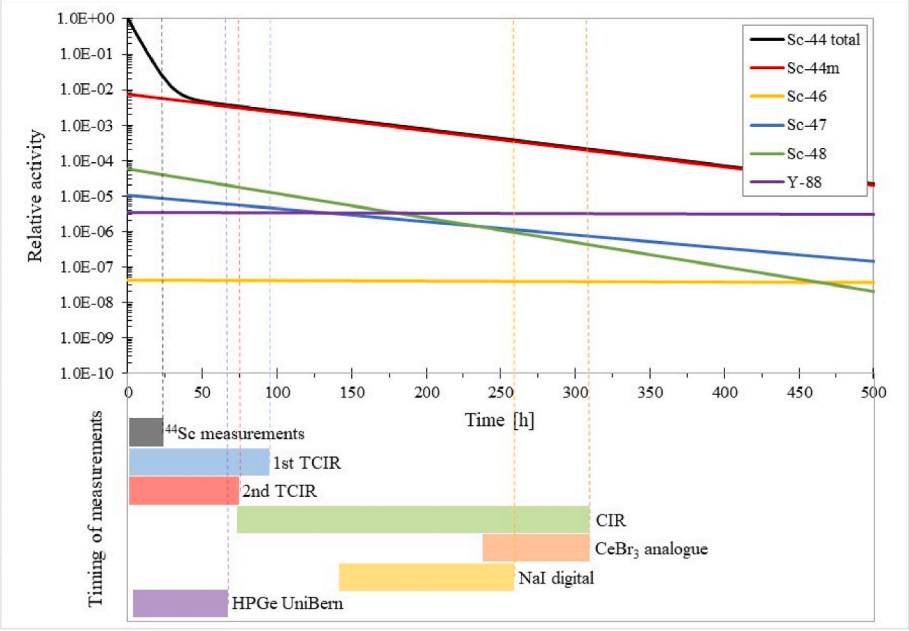

Fig. 4. On top, evolution of the relative amount of ^{44}Sc and the other radionuclides found in the solution. Below, under the same time scale, the timing of the measurements is shown. ^{44}Sc half-life measurements are all represented under the timeline delimited by the grey block, as they were done under a much shorter interval, and the other blocks indicate the different methods used to measure ^{44m}Sc half-life.

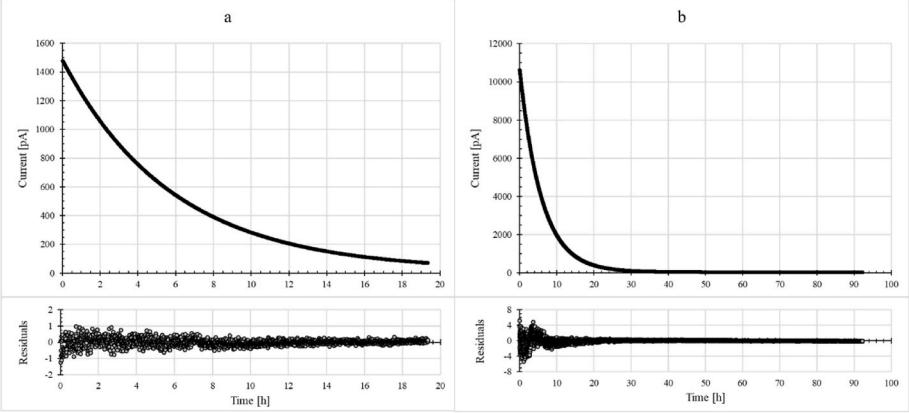

Fig. 5. Current over time measured with the TCIR at the beginning of the campaign in July 2021. **a**: First and shorter measurement from which ^{44}Sc half-life was obtained. **b**: Second and longer measurement from which both ^{44}Sc and ^{44m}Sc half-lives were obtained. The corresponding residuals of the fits using equation *(1)* for both datasets are presented below each decay curve.

$$I(t) = I_{44}(0) \bullet e^{-\lambda_{44}\bullet t} \bullet F_{dec} + I_{44m}(0) \bullet \left[e^{-\lambda_{44m}\bullet t} + \frac{\lambda_{44}}{\lambda_{44} - \lambda_{44m}} \bullet \left(e^{-\lambda_{44m}\bullet t} - e^{-\lambda_{44}\bullet t} \right) \right] + + I_{47}(0) \bullet e^{-\lambda_{47}\bullet t} + + I_{48}(0) \bullet e^{-\lambda_{48}\bullet t} \quad (2)$$

Decay constants for ^{47}Sc and ^{48}Sc were fixed using the recommended values of $\lambda_{47} = 2.3959(6)\cdot 10^{-6}$ s^{-1} and $\lambda_{48} = 4.408(10) \cdot 10^{-6}$ s^{-1} (Nucleide-LARA database). The initial currents were free parameters and turned out compatible with the estimated ratios in Table 1. The results in this case for ^{44}Sc and ^{44m}Sc half-lives were determined to be 4.0391(8) h and 58.6(2) h, respectively.

3.2. Measurements with the CIR

Two different measurements were performed using the CIR (*chambre d'ionization de référence*) (Juget et al., 2016) each one with the corresponding source prepared from the two solutions received. In order to measure the ^{44}Sc half-life starting on the day of receipt, the first source was monitored for almost 20 h, yielding 283 measurement points (Fig. 6). To calculate the half-life of ^{44}Sc, the fit of the data was performed using equation *(1)* fixing $\lambda_{44m} = 0.01183$ h^{-1}, as obtained in the previous section. The resulting value for ^{44}Sc half-life was determined to be 4.031(3) h.

The decay of the second source was measured three days after receipt. In this case, the measurements were performed in three parts, due to the intermittent availability of the chamber. The fit was performed according to equation (3) fixing the decay constants for ^{47}Sc, ^{48}Sc, ^{88}Y and ^{44}Sc, this last one from the value obtained in section 3.1 ($\lambda_{44} = 0.17161$ h^{-1}). The result for ^{44m}Sc half-life was determined at 58.81(5) h.

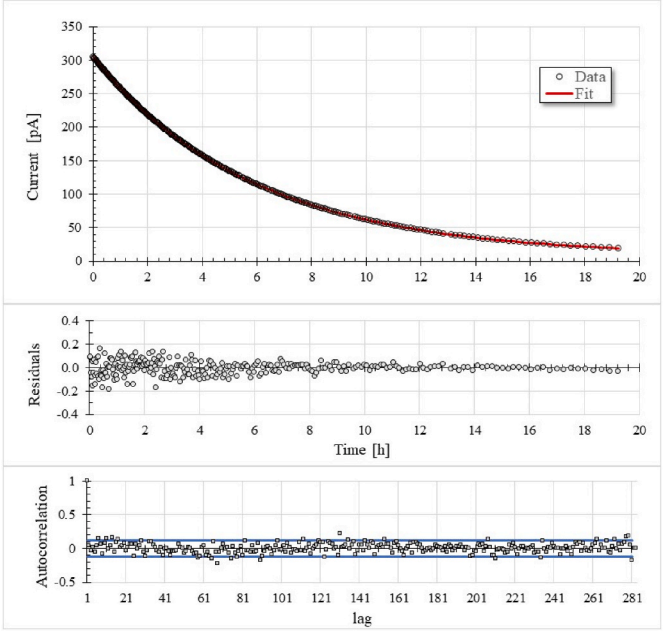

Fig. 6. Current decay curve measured with the CIR along with the fit curve, residuals and autocorrelation plot of the residuals to search for eventual medium or low frequency deviations in the residuals that might pass unnoticed (blue lines show the critical values for the autocorrelation function). (For interpretation of the references to colour in this figure legend, the reader is referred to the Web version of this article.)

$$I(t) = I_{44}(0) \bullet e^{-\lambda_{44}\bullet t} \bullet F_{dec} + I_{44m}(0) \bullet \left[e^{-\lambda_{44m}\bullet t} + \frac{\lambda_{44}}{\lambda_{44} - \lambda_{44m}} \bullet \left(e^{-\lambda_{44m}\bullet t} - e^{-\lambda_{44}\bullet t} \right) \right] + + I_{47}(0) \bullet e^{-\lambda_{47}\bullet t} + I_{48}(0) \bullet e^{-\lambda_{48}\bullet t} + I_{88}(0) \bullet e^{-\lambda_{88}\bullet t} \quad (3)$$

3.3. γ-spectrometry with a $CeBr_3$ detector

This measurement method was used previously at IRA when measuring the ^{175}Yb half-life (Durán et al., 2021). The γ-ray $CeBr_3$ detector is a Scionix 51B51/2M-CEBR-E1. It consists of a cylindrical 2x2-inch $CeBr_3$ crystal coupled to a photomultiplier tube, all within a shielded well topped with lead bricks. The signal from the preamplifier was shaped by means of a Canberra 2024 amplifier and then divided into two lines. One to be fed into an analogue electronic and the other into a digital electronic.

The analogue chain was composed of a Canberra 2037A single-channel analyser with pulse lockout logic minimising out-of-channel event dead-time. The pulses from this module were again duplicated, so that one line would undergo a 50 μs non-extending dead-time imposition and the other a 150 μs dead-time imposition. The dead-time was applied by combining an Ortec CO4020 input logic with a Philips 794 gate and delay generation. Both signals were sent to the integrated 32-bits counter/timer PCI-6602 device from National Instruments, to count the number of γ-rays above an energy threshold set in the single-channel analyzer.

Two measurements with different thresholds were performed. The first measurement was aimed at measuring the ^{44}Sc half-life, so a higher-energy threshold was set (364.5 keV, taking the ^{131}I peak as a reference) to eliminate low energy ^{44m}Sc emissions. This lasted 16 h in total, with 481 individual measurements of 120 s each. The second measurement was intended to measure the ^{44m}Sc half-life and, supposing there was no significative amount of unsupported ^{44}Sc left (from the target irradiation), the threshold was lowered to 22 keV, taking ^{109}Cd peak as a reference. It lasted for 71 h, acquiring 4269 points with individual measurements of 30 s at the beginning and 60 s at the end.

The number of counts on each channel was recorded using an automated acquisition LabVIEW™ program, together with the starting and counting time of each measurement. The high-stability frequency pulses from the DCF77 frequency standard type 860 (PTB webpage), with an accuracy of 10^{-8} for a 10-s measuring time, were used to calculate the counting time precisely.

For both datasets obtained with different imposed dead-times, the fits to calculate ^{44}Sc half-life were performed following equation (1) and substituting the currents by countrates (ρ). The values found were: 4.043 (4) h for the measurement with 50 μs dead-time and 4.045 (5) h for the measurement with 150 μs dead-time.

The equation used for the fit to obtain ^{44m}Sc half-life was the following:

$$\rho(t) = \rho_{44m}(0) \bullet e^{-\lambda_{44m}\bullet t} + \rho_{47}(0) \bullet e^{-\lambda_{47}\bullet t} + \rho_{48}(0) \bullet e^{-\lambda_{48}\bullet t} + \rho_{88}(0) \bullet e^{-\lambda_{88}\bullet t} + Bkg \quad (4)$$

In this case, the measurement started 10 days after the ^{44}Sc production, so that the equilibrium was already reached (Fig. 7) and the non-equilibrium equation contribution did not have to be taken into account. The initial countrates were free parameters in the fit, and half-life values for ^{47}Sc, ^{48}Sc and ^{88}Y were fixed to reference values Nucleide-LARA database (80.364 h, 43.67 h and 106.63 d). The ^{44}Sc half-life was fixed as well to the value of 4.04 h, as obtained from the previous fits. The result for ^{44m}Sc half-life is 59.0(2) h for the 50 μs dead-time measurement and 59.1(2) h for the 150 μs dead-time measurement.

The digital approach was performed using a National Instruments digitizer (NI 5772) linked to a FPGA module (NI PXIe-7975R) working at

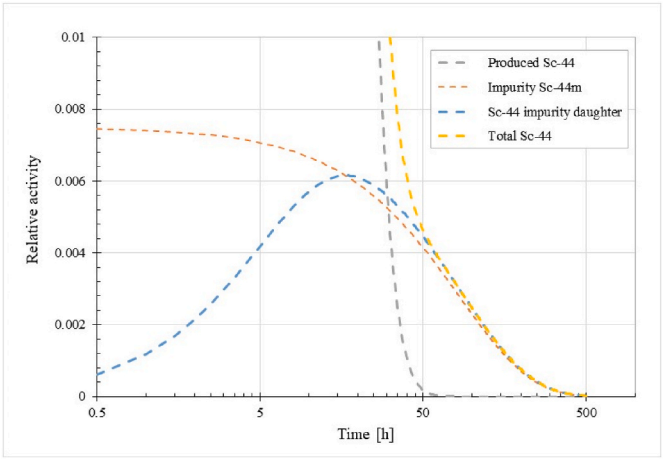

Fig. 7. Plot showing the decay of all ^{44}Sc and ^{44m}Sc contributions and the time they take reach to the equilibrium.

100 MS/s sampling frequency with 12-bit resolution. The timing and synchronization was achieved with a high-precision oscillator included in the timing control module NI PXIe-6672. Data acquisition and further data processing were performed with a custom-designed LabVIEW software application. More details about this system can be found in Durán et al. (2018).

The measurement was performed over an 11-h period (Fig. 8), collecting 750 points with increasing measurement duration ranging from 30 s to 120 s in order to obtain an adequate counting statistics. The fitting function was equation (*1*), again, substituting the current with countrate. To obtain the countrate, all events above a 22-keV energy threshold were counted. ^{44m}Sc decay constant was fixed to the previously-obtained value of $\lambda_{44m} = 0.0118\ h^{-1}$. The result for the ^{44}Sc half-life was 4.053(6) h.

3.4. γ-spectrometry with NaI(Tl) well detector

The same digital electronics described in the previous section was used to acquire and process the signal from another gamma detector. This device is a Quartz & Silica 127-SPE-127 12.5 × 12.5 cm NaI(Tl) well-type detector with a RTC type XP2050 photomultiplier, both housed within a cylindrical shielding. The source is inserted into the bottom of the well, interacting through 99.1% of the full solid angle.

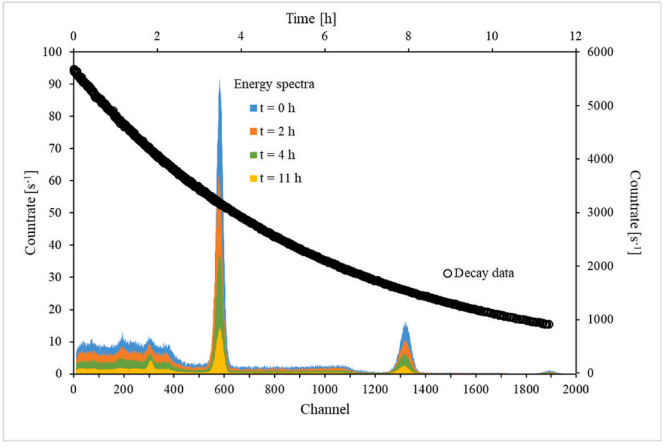

Fig. 8. Two plots are superposed on this figure: the energy spectra registered at different moments during the following of the decay (left and lower axes) and the decay curve, where each point represents the area of the corresponding spectrum, from the 22 keV threshold on, at the moment of measurement (right and upper axes).

The countrate decay of the source (Fig. 9) was followed over almost 92 h and 239 measurement points were obtained by counting the events above 22 keV for 60 s. Equation (4) was used in the fit, yielding 58.57(7) h for the ^{44m}Sc half-life value.

3.5. γ-spectrometry with the UniBern HPGe detector

The Eppendorf vial containing the scandium solution was inserted into a dedicated bottle and centered above the detector using a methacrylate piece that allows the fixing of the position of the source position at different distances from the detector (Fig. 10).

The detector is a N-type coaxial HPGe detector (Canberra GR2009) with the sensitive volume shielded by 10 cm of lead. The detector is coupled to a preamplifier and to a Lynx® digital signal analyzer and features the Genie2K analysis software and the Microsoft Excel application Excel2Genie (Forgács et al., 2014).

To calculate the half-lives two peaks were chosen, each one corresponding to the emission of each radionuclide: 271 keV for ^{44m}Sc and 1499 keV for ^{44}Sc. Thus, the decay of each radionuclide can be followed independently. The measurement was carried out for almost 70 h, giving 258 data points for the ^{44m}Sc peak and 229 for the ^{44}Sc peak, respectively. Individual measurement durations ranged between 770 and 900 s. The corresponding activities (as can be seen in Fig. 11) were calculated by dividing the countrates by the efficiency values from the detector's calibration and the reference emission probabilities: 0.00526 and 86.7% for the 271 keV emission and 0.00104 and 0.908% for the 1499 keV emission. Nevertheless, the fits were performed by simply using the countrates to avoid additional contributions to the uncertainty due to the efficiencies and emission probabilities.

To calculate the ^{44m}Sc half-life, a simple exponential decay equation was used for the fit:

$$\rho_{44m}(t) = \rho_{44m}(0) \bullet e^{-\lambda_{44m} \bullet t} \bullet F_{dec} + Bkg \tag{5}$$

For ^{44}Sc, one needs to account for the ^{44}Sc produced by the ^{44m}Sc. Here, λ_{44m} is a constant parameter equal to the value obtained in the previous fit: $\lambda_{44m} = 0.011831\ h^{-1}$.

$$\rho_{44}(t) = \rho_{44}(0) \bullet e^{-\lambda_{44} \bullet t} \bullet F_{dec} + \rho_{44m}(0) \bullet \frac{\lambda_{44}}{\lambda_{44} - \lambda_{44m}} \bullet \left(e^{-\lambda_{44m} \bullet t} - e^{-\lambda_{44} \bullet t}\right) + Bkg \tag{6}$$

Datasets and fit curves are presented in Fig. 11 with their corresponding residuals. In the case of the ^{44}Sc dataset, the data measured

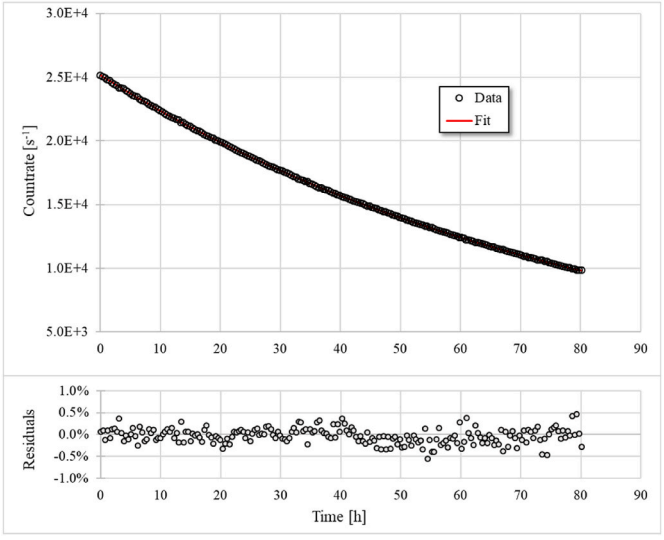

Fig. 9. Countrate decay measured with NaI(Tl) well-type detector with fit and corresponding residuals showing a medium frequency oscillation.

Fig. 10. Images from the source container, positioning system and detector enclosure at UniBern. From left to right: Eppendorf vial, bottle where the Eppendorf vial is inserted, detector enclosure and methacrylate positioning device.

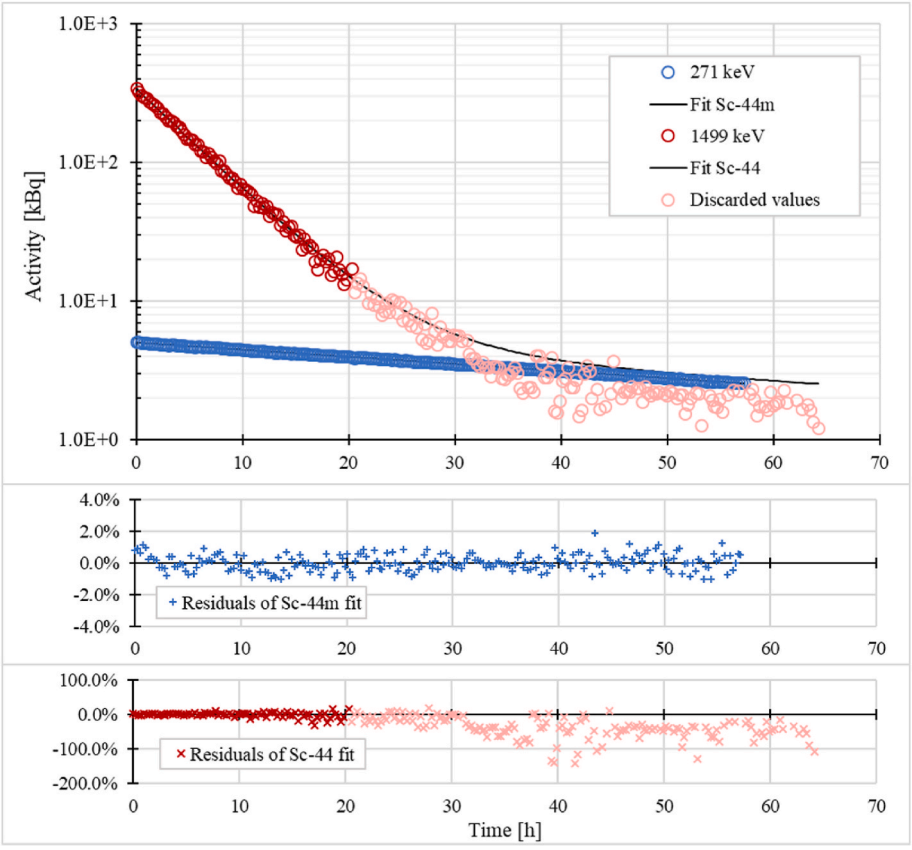

Fig. 11. Activities measured over time from the emission peaks of 271 keV and 1499 keV for ^{44m}Sc and ^{44}Sc. The fit curves are also represented with the datasets and below the residuals of the corresponding fits.

after 20 h (represented as pink circles in the plot) are not taken into consideration for the calculation of the half-life. At that point of the measurement, the counting statistics for the 1499 keV emission is low (under 100 counts under the peak) and, as can be observed in the plot, this has a direct impact on the reliability of the data to be used for the fit.

The values obtained for the half-lives were $T_{1/2}(^{44m}Sc) = 58.6(2)$ h and $T_{1/2}\ (^{44}Sc) = 4.05(2)$ h.

4. Half-life determination procedure and discussion

4.1. Uncertainty evaluation

The components are divided into high, medium and low frequency (Pommé et al., 2008).

- *High-frequency deviations*

For the CIR and TCIR measurements this component is evaluated by the standard deviation of the residuals, while for the γ-spectrometry measurements the counting statistics are evaluated. To obtain the uncertainty component, those values are multiplied by a propagation factor (Pommé and De Hauwere, 2020) that takes their impact over the whole observation of the decay into account:

$$f_{prop} = \frac{2}{\lambda \bullet T}\sqrt{\frac{3 \bullet (n-1)}{n \bullet (n+1)}} \tag{7}$$

where λ is the value obtained for the decay constant (half-life), T the duration of the whole observation of the decay and n the total number of

data points.

- *Medium-frequency deviations*

For medium-frequency deviations, the propagation factor is the same as in equation (7), but substituting n by the number of periods covered by the effect, considered as $= \frac{T}{T_{1/2}}$.

Medium-frequency deviations are identified as the perturbations due to the uncertainties in the impurity quantity and in their half-life values. For the half-life, the uncertainty values are those from the references (Nucleide-LARA database) and, for the quantity, is estimated from the HPGe spectrometry value presented in section 2.1, which is around 2%. The latter is expressed in the initial values for the current or countrate that appear in equations (1), (2) and (4): $I_{44m}(0), I_{47}(0), I_{48}(0)$ and $\rho_{44m}(0), \rho_{47}(0), \rho_{48}(0)$.

To propagate their uncertainties on the half-life calculation, the fit was performed taking the higher and lower values of these parameters (adding or substracting 2% of the value found in the fit). The two values obtained for the resulting half-life, a_+ and a_- are used in the following expression *(8)* to calculate the uncertainty component (σ_a) following a rectangular probability distribution, where all the values are equally probable between the higher and lower limits:

$$\sigma_a = \frac{(a_+ - a_-)}{2 \bullet \sqrt{3}} \tag{8}$$

- *Low-frequency deviations*

These sources of uncertainty are background and timing for all the methods and the uncertainty on the dead-time imposed for the $CeBr_3$ and NaI(Tl) measurements. In this case the propagation factor is just $f_{prop} = \frac{2}{\lambda \bullet T}$.

Table 2 presents the uncertainty budget in the calculation of the ^{44}Sc half-life for each measurement. For ^{44m}Sc, the uncertainty budget is made in a similar manner for each measurement.

The combined uncertainty for each measurement method is calculated as the square root of the sum of the components' squares.

In Table 3, to assess the final combined uncertainties, each uncertainty component is calculated as the mean from all the corresponding components from each individual measurement. In this compilation the standard deviation of the mean half-life value is also taken into account and is represented as "Mean".

4.2. ^{44}Sc half-life

The final value for the ^{44}Sc half-life was obtained as the arithmetic mean of all the values obtained for the different measurements. Fig. 12 shows all the individual values and their mean value: 4.042(7) h. The error bars are represented as the combined uncertainty values calculated individually for each measurement (as in Table 2) and the final combined uncertainty (as in Table 3) for the final value. The dotted lines represent the final combined uncertainty at $k = 1$ and $k = 2$, showing the compatibility of all results.

This value is compatible with the previous one published in 2016 by Garcia-Torano et al., but not with the evaluated reference from 2011 by Chen et al.. It should be noted that this reference value is the weighted mean of the three previous ones (Fig. 1) dating from 1966 by Tatarczuk and Medicus and 1969 by Sachdev and Yaffe and Ravn: 4.00(2) h, 4.05 (3) h and 3.927(8) h. The last measurement contributes to the mean with a bigger weight due to its significantly lower uncertainty (0.2%). In this case, the determination of ^{44}Sc half-life was done by least-squares fitting of a set of 20 points following the decay of the source, and corrected for impurities that stayed below 1–5%. The uncertainty evaluation included only the standard deviation of the residuals, so it may be underestimated.

Table 3
Uncertainty budget for the final values of ^{44}Sc and ^{44m}Sc half-lives.

Uncertainty components	^{44}Sc	^{44m}Sc
High-frequency		
Counting statistics	0.146%	0.093%
Residuals std. dev.	0.001%	0.007%
Medium-frequency		
Impurity	0.035%	0.014%
Impurity half-life	0.002%	0.011%
Low-frequency		
Background	0.013%	0.105%
Timing	0.067%	0.158%
Dead-time	0.030%	0.098%
Mean	0.070%	0.36%
Final combined uncertainty	**0.18%**	**0.43%**

4.3. ^{44m}Sc half-life

The ^{44m}Sc half-life was calculated in a similar manner. The arithmetic mean from the individual values is taken as the final half-life and the corresponding combined uncertainty budget is presented in detail in section 4.1. A summary of the values used to calculate the mean is presented in the following table (Table 4).

The values obtained from the measurement with the $CeBr_3$ detector are slightly higher than the rest. This is probably due to the high activity of the source, even at the moment of measurement (10 days after

Table 2
Uncertainty budgets for each measurement of the ^{44}Sc half-life.

Uncertainty components	TCIR 1st	TCIR 2nd	CIR	$CeBr_3$ analogue 50 & 150 μs	$CeBr_3$ digital	HPGe UniBern
High-frequency						
Counting statistics	–	–	–	0.0136%	0.018%	0.54%
Residuals std. dev.	0.0013%	0.0006%	0.0023%	–	–	–
Medium-frequency						
Impurity	0.036%	0.0028%	0.031%	0.0507%	0.038%	–
Impurity half-life	0.010%	0	0.0005%	0.0007%	0.0005%	0.0003%
Low-frequency						
Background	0.0003%	0.0001%	0.0006%	0.0102%	0.070%	–
Timing	0.072%	0.0190%	0.073%	0.0875%	0.124%	0.0067%
Dead-time	–	–	–	0.012% (50μs) 0.041% (150μs)	0.036%	–
Combined uncertainty	**0.082%**	**0.019%**	**0.079%**	**0.103%** (50μs) **0.110%** (150μs)	**0.153%**	**0.541%**

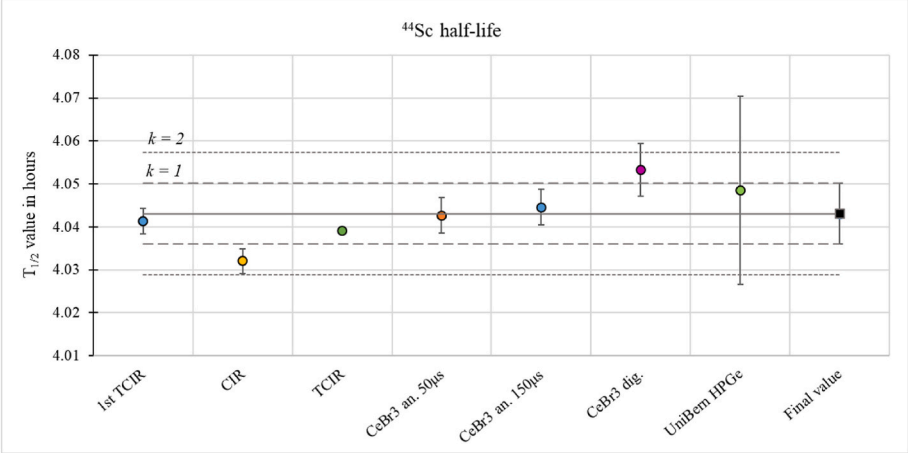

Fig. 12. Compilation of ^{44}Sc half-life values obtained from each measurement method, together with the arithmetic mean as the final result.

Table 4
Individual and final ^{44m}Sc half-life values.

Measurement method	TCIR 1st	TCIR 2nd	CIR	$CeBr_3$ analog	NaI(Tl) digital	HPGe UniBern
Individual value (hours)	58.6 (2)	58.6 (2)	58.8 (1)	59.0 (2) 59.1 (2)	58.9 (5)	58.6 (2)
Final value (hours)	**58.7 (3)**					

reception) that already caused some saturation problems at the first attempt of measurement. Nevertheless, they are compatible with the rest of measurements and, as a result, have been included in the calculation.

5. Conclusions

The half-life values for the decay of ^{44}Sc and ^{44m}Sc were determined as the mean value of 7 measurements with five different methods: portable ionization chamber, fixed ionization chamber, analogue γ-spectrometry with a $CeBr_3$ detector, γ-spectrometry with a HPGe detector and digital γ-spectrometry with a $CeBr_3$ detector for ^{44}Sc and with a NaI well-type detector for ^{44m}Sc. These new determinations are supported by multiple individual measurements by different methods and detailed uncertainty evaluations.

Several impurities had to be taken into account in the case of ^{44m}Sc and be corrected for. A plot showing the relative amount of these impurities as a function of time proved to be useful when considering which ones should be considered and when.

Our findings represent an improvement in the knowedge of ^{44}Sc properties and have a direct implication in the cyclotron production methodologies aimed at making this radionuclide widely available for nuclear medicine applications.

CRediT authorship contribution statement

M. Teresa Durán: Writing – original draft, Visualization, Validation, Software, Methodology, Investigation, Formal analysis, Data curation, Conceptualization. **Frédéric Juget:** Writing – review & editing, Writing – original draft, Validation, Resources, Methodology, Formal analysis, Data curation, Conceptualization. **Youcef Nedjadi:** Writing – review & editing, Supervision, Resources, Methodology, Conceptualization. **Claude Bailat:** Writing – review & editing, Supervision, Resources, Project administration, Methodology, Investigation, Formal analysis. **Pascal V. Grundler:** Writing – review & editing, Resources, Investigation. **Zeynep Talip:** Writing – review & editing, Resources, Investigation. **Nicholas P. van der Meulen:** Writing – review & editing, Resources, Project administration, Investigation, Conceptualization. **Pierluigi Casolaro:** Writing – review & editing, Resources, Methodology, Investigation, Data curation. **Gaia Dellepiane:** Writing – review & editing, Writing – original draft, Resources, Investigation, Formal analysis, Data curation. **Saverio Braccini:** Writing – review & editing, Supervision, Resources, Project administration, Methodology, Investigation, Conceptualization.

Declaration of competing interest

The authors declare that they have no known competing financial interests or personal relationships that could have appeared to influence the work reported in this paper.

Data availability

Data will be made available on request.

References

Andersson, G., 1954. LXIX. Electromagnetic separation of spallation products. Phil. Mag. 45, 621.
Browne, E., 2004. Table of radionuclides (Vol.1 – A=1–150), monographie BIPM-5. Bureau Int des Poids et Mesur. 45–50.
Chen, J., Singh, B., Cameron, J.A., 2011. Nuclear data sheets for A = 44. Nucl. Data Sheets 112, 2357–2495.
Dillman, L.T., Kraushaar, J.J., McCullen, J.D., 1963. The decay of Sc-44 and Sc-44m. Nucl. Phys. 42, 383–393.
Durán, M.T., et al., 2018. Fast digital 4πβ-4πγ coincidence counting system with offline analysis at IRA. Appl. Radiat. Isot. 134, 329–336.
Durán, M.T., et al., 2020. Determination of 161Tb half-life by three measurement methods. Appl. Radiat. Isot. 159, 109085.
Durán, M.T., et al., 2021. Ytterbium-175 half-life determination. Appl. Radiat. Isot. 176, 109893.
Forgács, A., Balkay, L., Trón, L., Raics, P., 2014. Excel2Genie: a Microsoft Excel application to improve the flexibility of the genie-2000 spectroscopic software. Appl. Radiat. Isot. 94, 77–81.
García-Toraño, E., et al., 2016. Standardisation and precise determination of the half-life of ^{44}Sc. Appl. Radiat. Isot. 109, 314–318.
Hibdon, Carl T., Pool, M.L., Kurbatov, J.D., 1945. Radioactive scandium I. Phys. Rev. 67, 289.
Juget, F., et al., 2016. Determination of ^{137}Cs half-life with a ionization chamber. Appl. Radiat. Isot. 118, 215–220.
Juget, F., et al., 2018. A portable precision ionization chamber: the transfer ionization reference chamber. Appl. Radiat. Isot. 134, 95–99.
Khurana, C.S., Hans, H.S., 1961. Cross-sections for (n, 2n) reactions at 14.8 MeV. Nucl. Phys. 28, 560.
Lima, T.V.M., et al., 2021. Fifty shades of Scandium: comparative study of PET capabilities using Sc-43 and Sc-44 with respect to conventional clinical radionuclides. Diagnostics 11, 1826.
Müller, C., et al., 2013. Promises of cyclotron-produced ^{44}Sc as a diagnostic match for trivalent β⁻-emitters: in vitro and in vivo study of a ^{44}Sc-DOTA-folate conjugate. J. Nucl. Med. 54, 2168–2174.

Nucleide-LARA database: basse de données atomiques et nucléaires Nucléide-LARA (LNHB, Laboratoire Nationale Henri Bécquerel) : http://www.lnhb.fr/donnees-nucleaires/module-lara/.
Pommé, S., Camps, J., Van Ammel, R., Paepen, J., 2008. Protocol for uncertainty assessment of half-lives. J. Radioanal. Nucl. Chem. 276 (2), 335–339.
Pommé, S., De Hauwere, T., 2020. Derivation of an uncertainty propagation factor for half-life determinations. Appl. Radiat. Isot. 158, 109046.
PTB. webpage. https://www.ptb.de/cms/en/ptb/fachabteilungen/abt4/fb-44/ag-442/dissemination-of-legal-time/dcf77.html.
Ravn, H., 1969. Yields and recoil properties of Scandium isotopes produced in the interaction of 590 MeV and 18 GeV protons with Uranium. J. Inorg. Nucl. Chem. 31, 1883–1890.
Rayburn, L.A., 1961. 14.4-Mev (n, 2n) cross sections. Phys. Rev. 122, 168.
Sachdev, D.R., Yaffe, L., 1969. Isomer ratios for the ^{44}Ca(p,n) ^{44}Sc^{m,g} and ^{85}Rb(p,n) ^{85}Sr^{m,g} reactions. Can. J. Chem. 47, 1667–1973.
Singh, A., et al., 2017. First-in-human PET/CT imaging of metastatic neuroendocrine neoplasms with cyclotron-produced ^{44}Sc-DOTATOC: a proof-of-concept study. Cancer Biother. Rad. 32 (4), 124–132.
Tatarczuk, J.R., Medicus, H.A., 1966. 44Sc isomeric yield ratios. Phys. Rev. 143 (3), 818–824.
van der Meulen, N.P., 2015. Cyclotron production of ^{44}Sc: from bench to bedside. Nucl. Med. Biol. 42, 745–751.
van der Muelen, N.P., et al., 2020. Developments toward the implementation of Sc-44 production at a medical cyclotron. Molecules 25 (20), 4706.
Waffler, H., Hirzel, O., 1948. Relative Wirkungsquerschnitte Fur Den (γ,n) Prozess mit der Lithium-Gamma-Strahlung (Quantenergie hv = 17.5 Mev). Helv. Phys. Acta 21, 200.